Laser and Particle Beams (2015), *33*, 109–115.

doi:10.1017/S0263034615000130

Electron acceleration by surface plasma waves in the presence of static magnetic field

PRASHANT CHAUHAN, DEEPIKA, ANSHU VARSHNEY, AND VIVEK SAJAL
Department of Physics and Material Science & Engineering, Jaypee Institute of Information Technology, Uttar Pradesh, India
(RECEIVED 27 October 2014; ACCEPTED 22 January 2015)

Abstract

Electron acceleration is studied during the resonant interaction of launched electron beam with the surface plasma wave (SPW) in the presence of static magnetic field. A configuration of two parallel metal sheets separated by a vacuum region supports the SPW of amplitude maximum on the two parallel interfaces and minimum in the middle. Kretschmann geometry is used to excite surface plasma mode by shinning laser on a glass prism. Dispersion relation of SPW is established in the presence of magnetic field and smaller cut-off frequencies are observed as compared with that of without magnetic field. An electron beam launched in the middle region, experiences a longitudinal ponderomotive force due to SPWs and gets accelerated to the velocity of the order of phase velocity of the surface wave. The energy gained by electron is higher in the presence of magnetic field as compared with zero magnetic field. The electron energy and trajectory are also presented for varying parameters such as amplitude of SPW and magnetic field strength. In the present scheme, electron beams can achieve maximum 550 KeV energy for the SPW amplitude $E_{SP} = 1.2 \times 10^{11}$ V/m, plasma frequency $\omega_p = 1.3 \times 10^{16}$ rad/s, and cyclotron frequency $\omega_c/\omega_p = 0.05$.

Keywords: Electron acceleration; Magnetic field; Surface plasma waves

1. INTRODUCTION

Electron acceleration has been the subject of research for many decades due to its wide applications ranging from high-energy physics to highly sensitive physical and chemical analyses (Yatsui, 1989). Tajima and Dawson (1979) analyzed that a laser beam propagating in plasma can excite electron plasma wave, which can be used to accelerate electrons. Since then tremendous progress is achieved, theoretically as well as experimentally in the laser-plasma interaction-based accelerators (Kawata *et al.*, 2005; Lifschitz *et al.*, 2006; Koyama *et al.*, 2006). The table top terawatt laser accelerators based on the chirped-pulse amplification technique are capable of producing high-energy electrons/protons in much shorter distances than the conventional accelerators due to the large electric fields, associated with lasers (Perry & Mourou, 1994; Hora *et al.*, 2000). The schemes of laser beat wave acceleration and laser wakefield acceleration have been studied rigorously in past two decades and electron acceleration upto GeV has been achieved using these schemes (Dawson, 1959; Hafizi *et al.*, 1997; Tomassini *et al.*, 2004; Tochitsky *et al.*, 2004; Jha *et al.*, 2013). However, in these accelerators, the laser intensities are very large (sometimes ultra-high laser intensities) due to which the accelerated electron energy is very high. The low-energy particle beams are expected to be useful for a wide range of contexts, including proton therapy for the treatment of cancers, materials characterization, radiation-driven chemistry, and in security application through the detection of explosives and narcotics.

One of the methods to generate well-behaved electron beams having low energy is electron acceleration by a surface plasma wave (SPW). This phenomenon was discovered recently and it was experimentally demonstrated that it is suitable for the production of relatively low-energy, quasi-monoenergetic electron beams with the usage of femtosecond lasers (Kupersztych *et al.*, 2001; Irvine *et al.*, 2004; Liu *et al.*, 2005). In this scheme, the evanescent electric field of surface plasmon polaritons accelerates photo-emitted electrons away from the surface. Zawadzka *et al.* (2000) used 150 fs, 6 μJ (21 GW/cm^2) laser pulses to excite SPWs using the Kretschmann configuration and demonstrated 40 eV electron production. In their follow-up experiments, 400 eV

Address correspondence and reprint requests to: P. Chauhan, Department of Physics and Material Science & Engineering, Jaypee Institute of Information Technology, Noida-201307, Uttar Pradesh, India. E-mail: prashant.chauhan@jiit.ac.in

electrons were generated by exciting the SPWs with 0.8 mJ (40 TW/cm^2) laser pulses (Zawadzka *et al.,* 2001). Kalmykov *et al.* (2006) have studied SPW excitation on two parallel plane silicon carbide films separated by a vacuum region and discussed its potential for electron acceleration. Steinhauer and Kimura (2003) developed an elegant analytical formalism for surface wave propagation over two parallel conducting planes and on the inner boundary of a hollow cylinder to describe the potential of SPW for electron acceleration. Later, Liu *et al.* (2007) used double-metal surface configuration separated by a vacuum region for studying electron acceleration, employing resonant interaction of electrons with SPW and achieved accelerating electrons up to tens of KeV energy. Dieckmann *et al.* (2002) examined electron acceleration by an electrostatic plasma wave in magnetized plasma. This energy of accelerated electrons can be further regulated by applying external magnetic field. An optimum static magnetic field should be applied to continuously accelerate electrons before entering the deceleration phase. The electron can gain and retain a significant energy in the form of cyclotron oscillations in the presence of a static magnetic field (Gupta & Suk, 2006; Sajal & Tripathi, 2008; Gupta *et al.*, 2014).

In this paper, we have studied the effect of static magnetic field applied in the direction of propagation of SPW on electron beam acceleration. To study this effect, we have used the configuration of two parallel metal surfaces that supports SPW having amplitude maxima on the two surfaces and minimum in the middle. This mode can be excited by shining a laser on the glass prism using the Kretschmann geometry Neuner *et al.* (2012). The static magnetic field is applied in the direction of propagation of SPW, that is, in the $\hat{z}$ -direction. When the axial velocity of the electron beam is comparable with that of the phase velocity of the surface wave, it can gain large energies from the wave. The applied magnetic field may be useful for accelerating electrons to achieve desired energies of moderate range with the control in their trajectories. The dispersion relation of SPW in double-metal surface configuration has been derived in Section 1 and electron acceleration by SPW has been discussed in Section 3. In Section 4, we have discussed the results and the conclusions in Section 5.

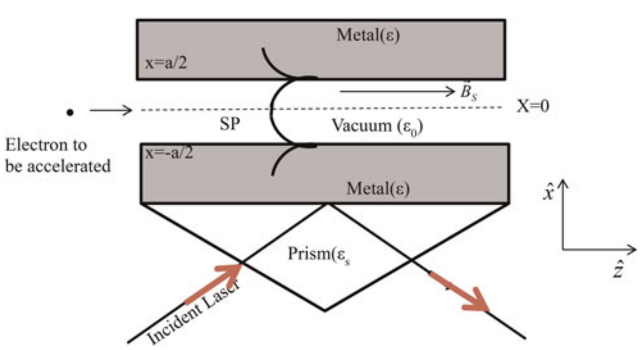

Fig. 1. Configuration of a vacuum bounded by the two metal surfaces.

2. SPW IN DOUBLE-METAL SURFACE CONFIGURATION

Consider two parallel metal half-spaces $x < -a/2$ and $x > a/2$ separated by a vacuum $-a/2 < x < a/2$ as shown in Figure 1. The SPW propagates along the $\hat{z}$-direction in this system. The electrons to be accelerated are injected in the center of the vacuum region and external axial magnetic field $\vec{B}_s$ is applied in the $\hat{z}$-direction. In this case, the effective permittivity ($\tilde{\varepsilon}$)of the metal is a dielectric tensor with independent components, each one as a function of frequency and the plasma's characteristics (Miraboutalebi *et al.*, 2012). It is given by

$$\tilde{\varepsilon} = \begin{pmatrix} \varepsilon_L - \dfrac{\omega_p^2}{\omega^2 - \omega_c^2} & \dfrac{i\omega_c}{\omega}\dfrac{\omega_p^2}{\omega^2 - \omega_c^2} & 0 \\ \dfrac{-i\omega_c}{\omega}\dfrac{\omega_p^2}{\omega^2 - \omega_c^2} & \varepsilon_L - \dfrac{\omega_p^2}{\omega^2 - \omega_c^2} & 0 \\ 0 & 0 & \varepsilon_L - \dfrac{\omega_p^2}{\omega^2} \end{pmatrix}, \quad (1)$$

where ε_L is the lattice permittivity, ω_p and ω_c are the plasma and cyclotron frequency. ω_c is computed as $\omega_c = eB_S/m$, where B_s is the strength of externally applied static magnetic field. The electric field of the SPW propagating through this configuration varies as Tochitsky *et al.* (2004). Maxwell's equations are used to study the dispersion relations of SPWs in this configuration.

$$\vec{\nabla} \times \vec{B} = \frac{1}{c^2}\frac{\partial}{\partial t}(\tilde{\varepsilon}\vec{E}), \quad (2)$$

$$\vec{\nabla} \times \vec{E} = -\frac{\partial \vec{B}}{\partial t}. \quad (3)$$

On eliminating $\vec{B}$ from Eqs (2) and (3), the wave equation can be found as

$$\vec{\nabla} \times \vec{\nabla} \times \vec{E} = \frac{\omega^2}{c^2}(\tilde{\varepsilon}\vec{E}). \quad (4)$$

Equation (4) can be expanded as follows:

$$\frac{\partial^2 E_x}{\partial x^2} - \left(k_z^2 - \frac{\omega^2}{c^2}\varepsilon_{xx}\right)E_x = 0, \quad (5a)$$

$$\frac{\partial^2 E_z}{\partial x^2} - \left(k_z^2 - \frac{\omega^2}{c^2}\varepsilon_{zz}\right)E_z = 0, \quad (5b)$$

where $\varepsilon_{xx} = \varepsilon_L - \omega_p^2/(\omega^2 - \omega_c^2)$ for $x > a/2$ and $x < -a/2$ and $\varepsilon_{xx} = 1$ for $-a/2 < x < a/2$ and $\varepsilon_{zz} = \varepsilon_L - \omega_p^2/(\omega^2$ for $x > a/2$ and $x < -a/2$, and $\varepsilon_{zz} = 1$ for $-a/2 < x < a/2$.

The electric field associated with the SPW [Eq. (5)] can be obtained by satisfying $\nabla . \tilde{\varepsilon}E = 0$ in each region, which are

https://doi.org/10.1017/S0263034615000130 Published online by Cambridge University Press

given by

$$E = \left[\frac{ik_z}{\alpha_1}\left(\frac{(\omega^2-\omega_p^2)(\omega^2-\omega_c^2)}{\omega^2(\omega^2-\omega_h^2)}\right)\hat{x}+\hat{z}\right]Ae^{-\alpha_1 x}.e^{-i(\omega t-k_z z)}, \quad \text{for } x > a/2, \tag{6a}$$

$$E = \left[\left(\frac{ik_z}{\alpha_2}\hat{x}+\hat{z}\right)A_1 e^{-\alpha_2 x} + \left(-\frac{ik_z}{\alpha_2}\hat{x}+\hat{z}\right)A_1' e^{\alpha_2 x}\right]e^{-i(\omega t-k_z z)}, \quad \text{for } -a/2 < x < a/2, \tag{6b}$$

$$E = \left[-\frac{ik_z}{\alpha_3}\left(\frac{(\omega^2-\omega_p^2)(\omega^2-\omega_c^2)}{\omega^2(\omega^2-\omega_h^2)}\right)\hat{x}+\hat{z}\right]A_2 e^{\alpha_1 x}e^{-i(\omega t-k_z z)}, \quad \text{for } x < -a/2, \tag{6c}$$

where $\omega_h^2 = \omega_p^2 + \omega_c^2$, $\alpha_1 = (k_z^2 - \omega^2\ \varepsilon_{zz}/c^2)^{1/2}$, $\alpha_2 = (k_z^2 - \omega^2/c^2)^{1/2}$, and $\alpha_3 = (k_z^2 - \omega^2\ \varepsilon_{xx}/c^2)^{1/2}$. A, A_1, A_1', and A_2 are constants. E_z and $\tilde{\varepsilon}E_x$ are continuous at the two interfaces $x = a/2$ and $x = -a/2$, which provides

$$Ae^{-\alpha_2 a/2} + A_1 e^{\alpha_2 a/2} - A_1' e^{-\alpha_1 a/2} = 0, \tag{7a}$$

$$Ae^{-\alpha_2 a/2} - A_1 e^{\alpha_2 a/2} - A_1'\left(\frac{\varepsilon_{zz}.\alpha_2}{\alpha_3}\right)e^{-\alpha_1 a/2} = 0, \tag{7b}$$

$$Ae^{\alpha_2 a/2} + A_1 e^{-\alpha_2 a/2} - A_2 e^{-\alpha_1 a/2} = 0, \tag{7c}$$

$$Ae^{\alpha_2 a/2} - A_1 e^{\alpha_2 a/2} + A_2\left(\frac{\varepsilon_{zz}.\alpha_2}{\alpha_3}\right)e^{-\alpha_1 a/2} = 0. \tag{7d}$$

On eliminating A, A_1, A_1', and A_2, we obtain the dispersion relation of the SPW in the presence of external magnetic field as

$$\frac{\alpha_2^2}{\alpha_3^2} = \left|\frac{1-e^{\alpha_2 a}}{1+e^{\alpha_2 a}}\right|^2 \frac{1}{\varepsilon_{zz}^2}. \tag{8}$$

Equation (8) is normalized using dimensionless quantities $q = k_z c/\omega_p$, $\Omega = \omega/\omega_p$, $\Omega_c = \omega_c/\omega_p$, and width of vacuum gap(a) is $a' = a\omega_p/c$. Figure 2 depicts the variation of the normalized distance between the metal plates ($a\omega_p/c$) versus electric field of SPW in the vacuum region for $k_z c/\omega_p = 0.05$. It is observed that the surface plasma modes exist on both metal surfaces with electric field minimum in the center and maximum on the two surfaces. Figure 3 shows variation of (ω/ω_p) versus $(k_z c/\omega)$ on the varying normalized cyclotron frequency (ω_c/ω_p) for the mode that has E_x symmetric about $x = 0$ $(A_1 = A_1')$. The parameters are $a' = 100$ and $\varepsilon_L = 1$. Recently, Liu *et al.* (2007) obtained dispersion relation of SPWs for double-metal surface configuration and observed linear increase in the frequency of SPWs with the wavenumber and it saturates at higher value

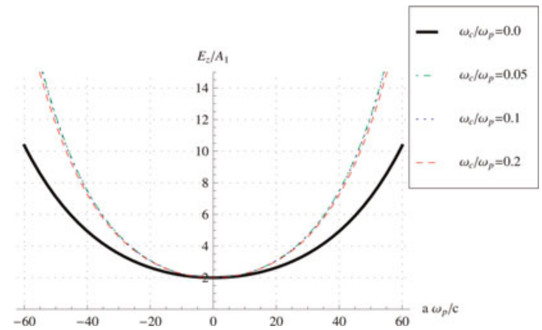

Fig. 2. Variation of the normalized distance between the metal plates ($a' = a\omega_p/c$) versus electric field of SPW.

of wavenumber that is, the wave propagates with frequencies ranging from zero at $(k_z c/\omega_p = 0)$ toward the asymptotic value $(\omega = \omega_p/\sqrt{2})$. In the presence of external magnetic field, the dispersion curve consists of two parts with a gap between them. One of the branches occurs at a higher frequency and the other at a lower frequency as shown in Figure 3. In the lower portion, the cut-off frequency occurs at $\omega = \omega_c$ and increases with the increase in cyclotron frequency. In the upper portion, the cut-off frequency decreases (enlarged view is shown in Figure 3b as the cyclotron frequency is varied from 0.05 to 0.2. Similar behavior is observed by Brion *et al.* (1972) and Chiu and Quinn (1972). We have studied electron acceleration for the lower portion at $k_z c/\omega_p = 0.04$. Figure 4 enveals the disersion relation of SPW on the varying distance between the two metal plates for $(\omega_c/\omega_p) = 0.2$ and $\varepsilon_L = 1$. It is observed that there is no effect on the dispersion characteristics of the SPWs with distance between the metal plates (Kumar *et al.*, 2010).

3. ELECTRON ACCELERATION IN THE PRESENCE OF A MAGNETIC FIELD

An electron beam is launched in the central region in the $\hat{z}$ -direction and static magnetic field $\vec{B}_s$ is applied in the same direction. This electron beam interacts with the wave of large amplitude in the central region ($E_z \cong 2.4 \times 10^{11}$ V/m at $x = 0$ as shown in Fig. 2). Although the field strength is less at the two interfaces, it is still sufficient for the electron acceleration. Zawadzka *et al.* (2001) reported that electric field amplitude of the order of 10^9 V/m can be used to accelerate electrons. Now, the motion of electrons is goverened by two fields, the electric field due to SPWs and the externally applied static magnetic field. The electron response is goverened by the equation of motion

$$m\frac{dv}{dt} = -e[(\vec{E} + \vec{v}\times\vec{B}) + (\vec{v}\times\vec{B}_s)], \tag{9}$$

where $-e$, m, and $\vec{v}$ are the electronic charge, mass, and velocity of the electron, respectively. We can replace the magnetic

https://doi.org/10.1017/S0263034615000130 Published online by Cambridge University Press

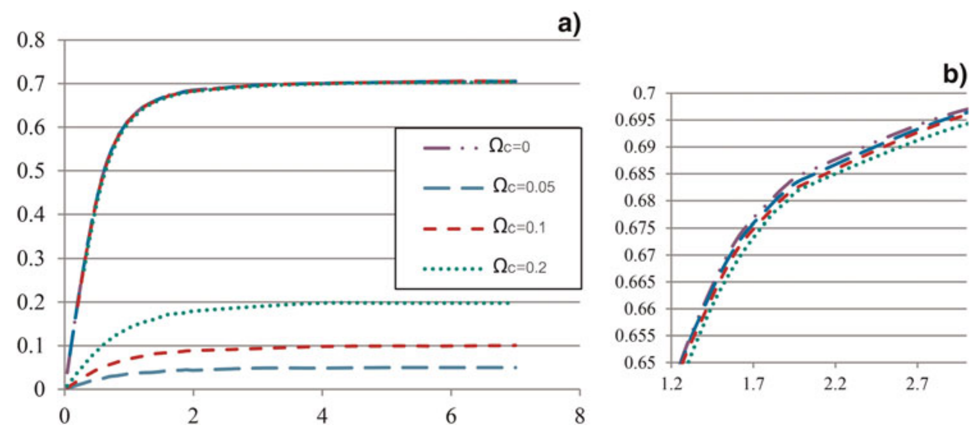

Fig. 3. (a) Variation of the normalized frequency (ω/ω_p) versus normalized wave number ($k_z c/\omega_p$). (b) Enlarged view of Figure 3a.

field of SPW by

$$\vec{B} = \frac{\nabla \times \vec{E}}{i\omega}.$$

Equation (9) is solved for x, y, and z-components of momentum of electron, which are given as

$$\frac{dp_x}{dz} = A_1\left[\frac{em\gamma}{p_z}\left(\frac{k_z}{\alpha_2}\right) - \frac{e}{\omega}\left(\frac{k_z^2}{\alpha_2} - \alpha_2\right)\right](e^{\alpha_2 x} + e^{-\alpha_2 x})\sin(\omega t - kz + \varphi) - \frac{e p_y B_s}{p_z}, \tag{10}$$

$$\frac{dp_y}{dz} = e\frac{p_x}{p_z}B_s \tag{11}$$

$$\frac{dp_z}{dz} = A_1\left[-\frac{me\gamma}{p_z}(e^{\alpha_2 x} - e^{-\alpha_2 x})\cos(\omega t - kz + \phi) + \frac{p_x}{p_z}\frac{e}{\omega}\left(\frac{k_z^2}{\alpha_2} - \alpha_2\right)\times (e^{\alpha_2 x} + e^{-\alpha_2 x})\sin(\omega t - kz + \phi)\right], \tag{12}$$

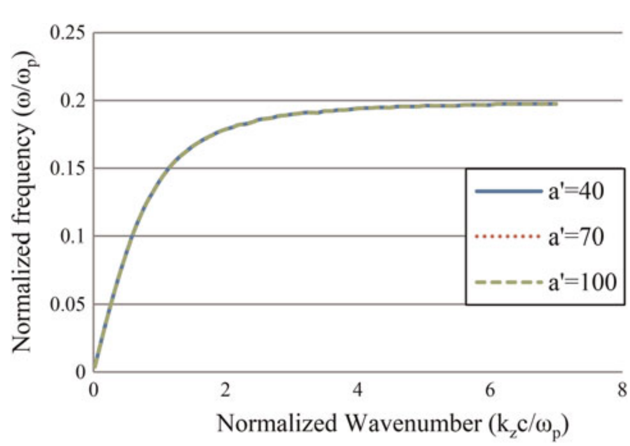

Fig. 4. Plot of dispersion relation of SPW on the varying distance between the metal plates ($a' = a\omega_p/c$) for ω_c/ω_p=0.2.

where $\gamma = (1 + (p_x^2 + p_y^2 + p_z^2/m^2 c^2))^{1/2}$ and ϕ is the initial phase of the wave. These equations are supplemented with

$$\frac{dx}{dz} = \frac{p_x}{p_z}, \tag{13}$$

$$\frac{dy}{dz} = \frac{p_y}{p_z}, \tag{14}$$

$$\frac{dt}{dz} = \frac{\gamma m}{p_z}. \tag{15}$$

The sets of Eqs (10)–(15) are normalized by introducing dimensionless quantities $A_1'' \rightarrow eA_1/m\omega_p c$, $X \rightarrow \omega_p x/c$, $Y \rightarrow \omega_p y/c$, $Z \rightarrow \omega_p z/c$, $P_x \rightarrow p_x/mc$, $P_y \rightarrow p_y/mc$, $P_z \rightarrow p_z/mc$, $T \rightarrow \omega_p t$, $\Omega \rightarrow \omega/\omega_p$, $\Omega_c \rightarrow \omega_c/\omega_p$, and $q \rightarrow k_z c/\omega_p$ and are solved numerically for the electron energy and electron trajectory. The parameters are $P_x(0) = 0.01$, $P_y(0) = 0.01$, $P_z(0) = 0.09$, $x(0) = 0.01$, $y(0) = 0.01$, $t(0) = 0.0$, $\phi = \pi/2$, $E_{SP} = 1.2 \times 10^{11}$ V/m, $\omega_p = 1.3 \times 10^{16}$ rad/s, and the width of vacuum gap is $a = 231$ μm, that is, $(a\omega_p/c) = 100$. The parameters used for this numerical analysis, are in agreement with the parameters used in the experimental and analytical studies by Zawadzka *et al.* (2001), Liu *et al.* (2007), Neuner *et al.* (2012), and Kumar *et al.* (2010). The kinetic energy gained by electrons with normalized distance have been ploted in Figure 5, with and without magnetic field. Figure 6 shows the effect of amplitude variation on electron energy. Trajectory of the electron beam has been plotted in Figures 7 and 8, respectively, on the varying magnetic field and amplitude of the wave.

4. RESULTS AND DISCUSSION

In Figure 5, we have plotted the energy (in KeV) gained by the electrons versus normalized distance ($z\omega_p/c$) for the increasing values of the normalized cyclotron frequency (ω_c/ω_p). It is observed that the electron acceleration is higher in the presence of an external magnetic field as

https://doi.org/10.1017/S0263034615000130 Published online by Cambridge University Press

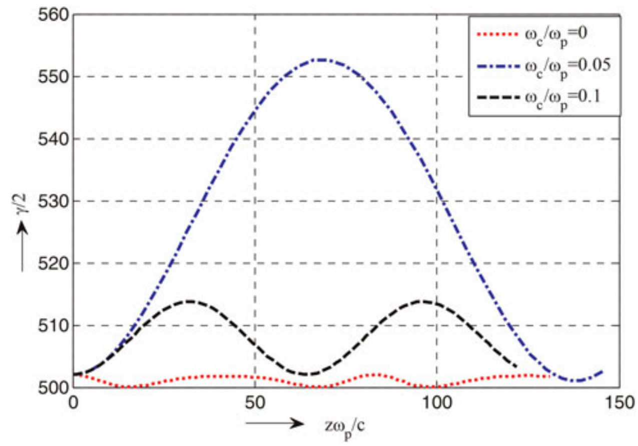

Fig. 5. Plot of kinetic energy ($\gamma/2$) in KeV gained by electron versus normalized distance ($z\omega_p/c$) on the varying strength of the magnetic field.

compared with that of without magnetic field. We have obtained electrons of energy $\approx$550 KeV for the cylotron frequency $(\omega_c/\omega_p) = 0.05$. On increasing (ω_c/ω_p) to 0.1, energy gained by electrons decreases to 512 KeV as compared with its values for $(\omega_c/\omega_p) = 0.05$, which is larger as compared with energy ($\approx$502 KeV) when the external magnetic field is zero. Electron gains energy during the rising part of the pulse and loses it during the trailing part, resulting in negligible energy gain. The presence of static magnetic field not only leads to the enhancement of the energy gain, but also to the retention of most of the energy in the form of cyclotron oscillations. The launched electron experiences a $V \times B$ force, which deviates it away from the axis either in the $+\hat{x}$ or $-\hat{x}$-direction, strikes the metal–vacuum interface (as shown in Fig. 7) and gains very small energy. On introducing external magnetic field, electron experiences another $V \times B_s$ force. This force prevents the electrons from escaping the SPW field and faces higher values of SPW amplitude, as it has maximum values at the two

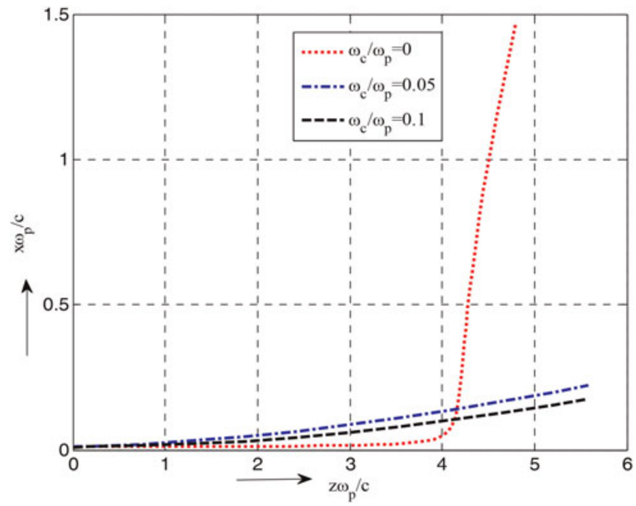

Fig. 7. Trajectory of the accelerated electron versus normalized distance on the varying strength of the magnetic field.

interfaces and minimum in the middle. The energy gained by the electron beam is more in the presence of an external field as compared with that of without field. With the increase in the strength of field, the electrons turn toward the z-axis more effectively and repeatedly, faces smaller values of SPW amplitude and hence their gain reduces. However, the gain is still more as compared with the energy gain in the absence of magnetic field. These results can be explained by Figure 5. In Figure 6, we have plotted energy (in KeV) gained by the electrons versus normalized distance ($z\omega_p/c$) for different values of SPW amplitude at $(\omega_c/\omega_p) = 0.2$. Energy gained by electron increases with the amplitude of SPW. Electron beam of energy ~550 KeV is obtained for SPW amplitude $eA_1/m\omega_p c = 0.02164$. Energy gained by electron beam decreases on decreasing the amplitude of SPW by two times, that is, for 0.01082 and 0.00541. The trajectories of the accelerated electrons launched in the center of the vacuum region are plotted in Figures 7–9. It is observed

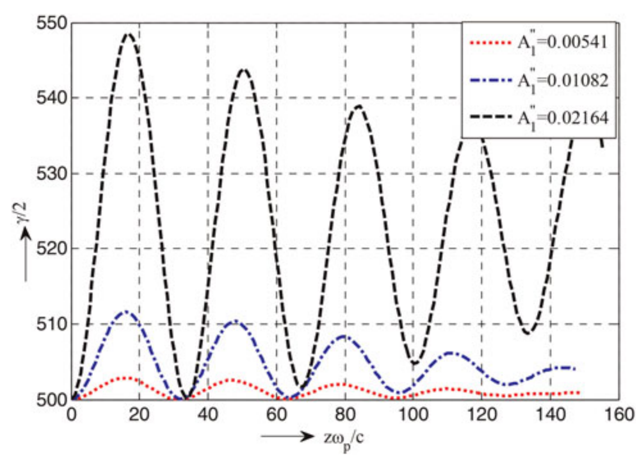

Fig. 6. Plot of kinetic energy ($\gamma/2$) in KeV gained by electron versus normalized distance ($z\omega_p/c$) for $(\omega_c/\omega_p) = 0.2$ on the varying amplitude of SPW.

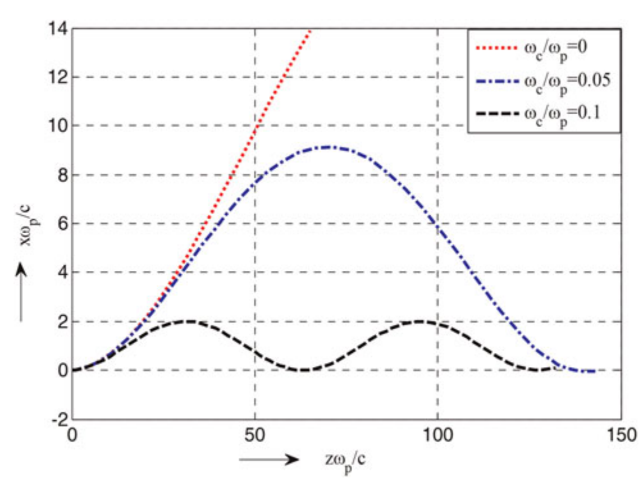

Fig. 8. Trajectory of the accelerated electron on the varying strength of the magnetic field.

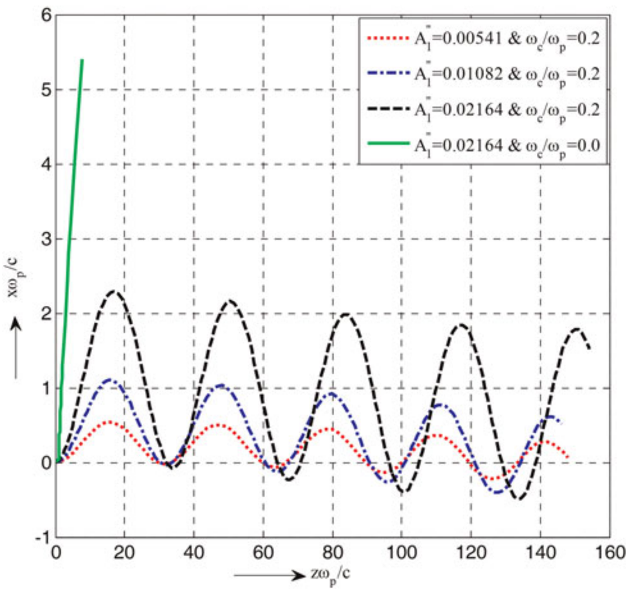

Fig. 9. Trajectory of the accelerated electron on increasing amplitude of SPWs when $(\omega_c/\omega_p) = 0.2$ and $(\omega_c/\omega_p) = 0.0$.

in Figure 7 that when $(\omega_c/\omega_p) = 0$, the electron beam travels along $x = 0$, that is, in straight line for the smaller values of $z\omega_p/c \simeq 4$ [Figure 7 of Liu *et al.* (2007)] and diverges strongly for the higher values of normalized distance. In the presence of external magnetic field, the electron experience $V \times B_s$ force and converges toward the positive z-axis. The electron beam converges more and more in the $\hat{z}$-direction on increasing (ω_c/ω_p) from 0.05 to 0.1 as shown in Figure 8. In the absence of magnetic field, the divergence of electron trajectory is much higher. Amplitude of SPW also affects electron trajectory significantly as shown in Figure 9.

5. CONCLUSIONS

Electron acceleration at moderate relative intensity by SPW excited with double-metal surface configuration shows a significant promise. The double-metal structure helps in guiding the electron beam without diverging it as the field of SPW is maximum at the two interfaces and minimum at the center. The electron beam injected in the center of the vacuum region follows nearly a straight line path in the absence of magnetic field, do not return to the axis and gains very small energy. An electron moving away from the $\hat{z}$-axis either in the $+\hat{x}$ or $-\hat{x}$-direction in the presence of magnetic field will experience a $V \times B_s$ force along the positive $\hat{z}$ -direction. This force prevents the electrons from escaping the SPW field and the electron returns to the axial points, hence gains energy. With an increase in strength of the magnetic field, the electrons turn toward the z-axis more effectively and repeatedly and gains less energy as it encounters lesser values of SPW amplitude in the central region. On increasing the amplitude of SPW, energy gain and trajectory of the accelerated electrons are further improved.

In conclusion, as the energy gained by the electron beam increases on applying external magnetic field as well as is affected by SPW amplitude and the electron trajectory is also connected with these two parameters, one can get a well-behaved moderate energy gain with controlled trajectory by optimizing these external parameters. This scheme is viable to achieve the beams of KeV energy for the optimum values of magnetic field and SPW amplitude.

REFERENCES

Brion, J.J., Wallis, R.F., Hartstein, A. & Burstein, E. (1972). Theory of surface magnetoplasmons in semiconductors. *Physical Review Letters* **28**, 22.

Chiu, K.W. and Quinn, J.J. (1972) Magneto-plasma surface waves in solids. *IL Nuovo Cimento* **10**, 1.

Dawson, J.M. (1959). Nonlinear electron oscillations in a cold plasma. *Phys. Rev.* **113**, 383–387.

Dieckmann, M.E., Ljung, P., Ynnerman, A. and McClements, K.G. (2002). Three-dimensional visualization of electron acceleration in a magnetized plasma. *IEEE Trans. Plasma Sci.* **30**, 20–21.

Gupta, D.N., Gopal, K., Nam, I.H., KULAGIN, V.V. and SUK, H. (2014). Laser wakefield acceleration of electrons from a density-modulated plasma. *Laser Part. Beams* **32**, 449–454.

Gupta, D.N. and Suk, H. (2006). Combined role of frequency variation and magnetic field on laser electron acceleration. *Phys. Plasmas* **13**, 013105.

Hafizi, B., Ting, A., Esarey, E., Sprangle, P. and Krall, J. (1997). Vacuum beat wave acceleration. *Phys. Rev. E* **55**, 5924.

Hora, H., Hoelss, M., Scheid, W., Wang, J.X., Ho, Y.K., Osman, F. and Castillo, R. (2000). Principle of high accuracy for the nonlinear theory of the acceleration of electrons in a vacuum by lasers at relativistic intensities. *Laser Part. Beams* **18**, 135–144.

Irvine, S.E., Dechant, A. and Elezzabi, A.Y. (2004). Generation of 0.4 keV femtosecond electron pluses using impulsively excited surface plasmons. *Phys. Rev. Lett.* **93**, 184801.

Jha, P., Saroch, A. and Mishra, R.K. (2013). Wakefield generation and electron acceleration by intense super-Gaussian laser pulses propagating in plasma. *Laser Part. Beams* **31**, 583–588.

Kalmykov, S., Polomarov, O., Korobkin, D., Otwinowski, J., Power, J. and Shvets, G. (2006). Novel techniques of laser acceleration: from structures to plasmas. *Philos. Trans. R. Soc. Lond., Ser. A* **364**, 725.

Kawata, S., Kong, Q., Miyazaki, S., Miyauchi, K., Sonobe, R., Sakai, K., Nakajima, K., Masuda, S., Ho, Y.K., Miyanaga, N., Limpouch, J. and Andreev, A.A. (2005). Electron bunch acceleration and trapping by ponderomotive force of an intense short-pulse laser. *Laser Part. Beams* **23**, 61–67.

Koyama, K., Adachi, M., Miura, E., Kato, S., Masuda, S., Watanabe, T., Ogata, A. and Tanimoto, M. (2006). Monoenergetic electron beam generation from a laser-plasma accelerator. *Laser Part. Beams* **24**, 95–100.

Kumar, P., Kumar, M. and Tripathi, V.K. (2010). Excitation of terahertz plasmons eigenmode of a parallel plane guiding system by an electron beam. *J. Appl. Phys.* **108**, 123303.

Kupersztych, J., Monchicourt, T.P. and Raynaud, M. (2001). Ponderomotive acceleration of photoelectrons in surface plasmon-assisted multiphoton photoelectric emission. *Phys. Rev. Lett.* **86**, 5180–5183.

Lifschitz, A.F., Faure, J., Glinec, Y., Malka, V., and Mora, P. (2006). Proposed scheme for compact GeV laser plasma accelerator. *Laser Part. Beams* **24**, 255–259.

Liu, C.S., Kumar, G., Singh, D.B. and Tripathi, V.K. (2007). Electron acceleration by surface plasma waves in double metal surface structure. *J. Appl. Phys.* **102**, 113301.

Liu, H., He, X.T. and Hora, H. (2005). Additional acceleration and collimation of relativistic electron beams by magnetic field resonance at very high intensity laser interaction. *Appl. Phys. B, Lasers Opt.* **82**, 93–97.

Miraboutalebi, S., Rajaee, L. and Matin, L.F. (2012). Surface wave excitations on magnetized over-dense plasma. *J. Theor. Appl. Phys.* **6**, 9.

Neuner III., B., Korobkin, D., Ferro, G. and Shvets, G. (2012). Prism coupled surface wave accelerator based on silicon carbide. *Phys. Rev. Spec. Top. – Accel. Beams* **15**, 031302.

Perry, M.D. and Mourou, G. (1994). Terawatt to petawatt sub picoseconds lasers. *Science* **264**, 917–924.

Sajal, V. and Tripathi, V.K. (2008). Large amplitude lower hybrid wave driven by laser and its effect on electron acceleration in a magnetic plasma channel. *Opt. Commun.* **281**, 3542–3546.

Steinhauer, L.C. and Kimura, W.D. (2003). Slow waves in microchannel metal waveguides and application to particle acceleration. *Phys. Rev. Spec. Top. – Accel. Beams* **6**, 061302.

Tajima, T., and Dawson, J.M. (1979). Laser electron accelerator. *Phys. Rev. Lett.* **43**, 267–270.

Tochitsky, S.Y., Narang, R., Filip, C.V., Musumeci, P., Clayton, C.E. and Yoder, R.B. (2004). Enhanced acceleration of injected electrons in a laser-beat-wave-induced plasma channel. *Phys. Rev. Lett.* **92**, 095004.

Tomassini, P., Galimberti, M., Giulietti, A., Giulietti, D., Gizzi, L.A., Labate, L. and Pegoraro, F. (2004). Laser wake field acceleration with controlled self-injection by sharp density transition. *Laser Part. Beams* **22**, 423–429.

Yatsui, K. (1989). Industrial applications of pulse power and particle beams. *Laser Part. Beams* **7**, 733–741.

Zawadzka, J., Jaroszynski, D., Carey, J.J. and Wynne, K. (2000) Evanescent-wave acceleration of femtosecond electron bunches. *Nucl. Instrum. Methods A* **445**, 324–328.

Zawadzka, J., Jaroszynski, D., Carey, J.J. and Wynne, K. (2001). Evanescent-wave acceleration of ultrashort electron pluses. *Appl. Phys. Lett.* **79**, 2130–2132.